Tuned vibration absorber for suppression of rest tremor in Parkinson's disease

S. M. Hashemi[1] **M. F. Golnaraghi**[2] **A. E. Patla**[3]

[1]Department of Mech., Aerospace & Ind. Eng., Ryerson University, Toronto, Canada
[2]Department of Mechanical Engineering, University of Waterloo, Waterloo, Canada
[3]Department of Kinesiology, University of Waterloo, Waterloo, Canada

Abstract—*A simple approach for the suppression of the tremor associated with Parkinson's disease is presented. The proposed system is a tuned vibration absorber (TVA), which has been very effective in the suppression of vibrations in an experimental model of the human arm with two degrees of freedom. Theoretical and numerical methods were used to study the behaviour of the arm model and to develop an effective tremor reduction approach. Based on these studies, a vibration absorber was designed, tested numerically and fabricated for experimental testing. Experimental investigations indicated that optimum control performance was related to the position of the controller and the excitation frequency. With a distance of 160 mm from the end of forearm, the TVA was found to have the best performance, and, for different tremor frequencies, the vibration of the experimental model was reduced by more than 80%.*

Keywords—*Parkinson's tremor, Passive vibration control, Tuned vibration absorbers*

Med. Biol. Eng. Comput., 2004, **42**, 61–70

1 Introduction

SINCE THE 1817 descriptions of 'shaking palsy' by James Parkinson (PARKINSON, 1817), the concept of the clinical entity Parkinson's disease (PD) has been established. The most prominent tremor in Parkinson's disease is rest tremor (i.e. when voluntary muscle activity is absent), although postural (i.e. provoked by the maintenance of posture) and movement tremors (i.e. provoked by any form of movement) are occasionally observed in these patients. Tremor can be characterised in terms of frequency, amplitude and waveform. The frequency of PD tremor varies from 2 to 10 Hz (GRIFFIN, 1990).

Because the underlying physiology of pathological tremor is not well understood, existing physical and drug therapies have not been successful in tremor treatment, giving rise to the need for alternative approaches to the problem of tremor suppression. To date, most technologies available for tremor control comprise so-called active and semi-active devices, such as those using electrical stimulation.

PROCHAZKA *et al.* (1992) proposed closed-loop functional electrical stimulation (FES) to activate tremorogenic muscles out-of-phase, thereby counteracting the tremor. The FES glove has electrical connections that are adapted to make electrical contact with skin electrodes on the user. A displacement signal, monitored by a sensor, is filtered to tune to the tremor frequency at the wrist. The glove can permit a user of reduced motor ability to grip objects.

HALL (1996) invented a hand-held gyroscopic device to attenuate the effects of tremors. In this invention, a gyroscope is firmly held against the back of the human hand to reduce or eliminate the effects of tremors. A DC motor powered by batteries drives the gyroscope. The batteries are mounted on the rotating part of the gyroscope and enhance the gyroscopic action. The gyroscope can hold the hand steady enough to allow a patient to perform a simple task. ARNOLD and ROSEN (1993) applied-energy-dissipating orthosis for people disabled by pathological intention tremor. The controlled energy-dissipating orthosis generates resistive loads by means of magnetic damping.

An active force feedback control device, incorporating a torsion spring, torque motor, accelerometer and microprocessor, was developed by REPPERGER (1989). Tremors or other undesired movements are sensed by an accelerometer. A control signal is output to the driving motor and torsion spring to oppose the tremor. ROSEN (1986) invented a viscous damping tremor suppression device that is applied to a wheelchair and is capable of suppressing vibrations during wheelchair operation. It includes a chamber filled with a viscous fluid, a position-sensing actuator assembly and a damping element disposed within the chamber. To suppress tremors, the damping characteristics are chosen selectively to reduce the amplitude of movements at or above 3 Hz.

In this paper, passive control of the rest tremor of the human arm, caused by PD, is addressed. The dynamic modelling of the arm is presented and numerically simulated in time and

Correspondence should be addressed to Prof. M. F. Golnaraghi; email: mfgolnar@uwaterloo.ca

Paper received 28 November 2002 and in final form 15 September 2003

MBEC online number: 20043843

frequency domains. Using the numerical simulation, a tuned vibration absorber (TVA) is then designed. Owing to its design simplicity and ease of manipulation, the TVA is considered to be advantageously useable for PD tremor control. The system is then tested on an experimental model. Experimental study is carried out to find the optimum absorber location on the experimental arm.

1.1 *Different vibration suppression strategies*

There are essentially two main approaches to forced vibration control: vibration isolation and vibration absorption. Vibration isolation is rather intuitive and has been around since vibration became an issue. The vibration isolation system is designed to isolate the source of vibration from the system of interest or to isolate the device from the source of vibration (KARNOPP, 1995). This can be done by using highly damped materials, such as rubber, to change the stiffness and damping between the source of vibration and the structure that is to be protected from the vibrations. Vibration isolation has been used widely in many fields, e.g. the design of automotive suspensions, seismic isolation platforms and rotating machinery. A theoretical study on PD tremor isolation was also reported by LI (2000). A human arm model with seven degrees of freedom for predicting arm movement and for designing the controller was developed. Transformation co-ordinate matrices were constructed to express the kinematics of the system. The Lagragian dynamics was used to arrive at the equations of motion. Experimental measurements were also carried out to validate the dynamic model (LI, 2000).

Here, a vibration control approach, based on vibration absorption, is proposed to suppress PD tremor of the human arm. Vibration absorption is often confused with vibration isolation. Vibration absorbers, however, are normally used to absorb or extract vibrations from an oscillatory system by adding a physical spring-mass-damper system to the structure (SUN *et al.*, 1995). By changing the absorber's characteristics, the added absorber's natural frequency can be tuned so that the structure does not feel the transmitted force. Research in vibration absorbers has yielded several fundamental designs. Among these are tuned vibration absorbers, Lanchester dampers and impact dampers. These designs utilise certain combinations of passive mechanical elements (springs and dampers) to reduce the vibration amplitude of a system. With recent advances in motion sensing and actuating, the design of vibration absorbers that utilise actively actuated elements has become more attractive (NAGAYA *et al.*, 1999).

A vibration absorber consists of a second mass-spring-damper combination added to the vibrating arm to reduce the amplitude of vibrations. The added system is called the absorber. Theoretically, the natural frequency of the vibration absorber can be tuned such that the amplitude of vibration is minimised at the frequency of vibration. The spring of the vibration absorber transfers vibration energy to added mass. This results in substantial motion of the added mass. A viscous damper is used to dissipate the energy of the vibration. The damper can usually reduce the amplitude of the added mass. At its resonance, the absorber drives the structure to impede structural motion. Low damping of an absorber results in improved performance for a given mass. In practice, however, damping is incorporated to maintain a reasonable trade-off between the absorber mass and its displacement. Damping also improves the effective frequency range of the operation of a vibration absorber.

In PD tremor, different patients have individual tremor frequencies (from 2 to 12 Hz). Therefore tremor suppression is a broadband vibration control problem. It is necessary that the proposed vibration absorber be tuned to suppress the tremor at a specific frequency. In the present study, we propose to use tuned vibration absorbers (TVAs), also called tuned mass dampers (TMDs), and dynamic vibration absorbers (DVAs) to reduce the amplitude of tremor in the human arm. The proposed control methods are based on the simultaneous consideration of energy dissipation and energy transfer in vibration systems.

The optimum vibration absorber design for a single-mass system has been designed by INMAN (1996). For a multi-degree-of-freedom system, SETO and TAKITA (1984) proposed the modal control theory. Once the vibration system is decoupled in the modal co-ordinate, this approach essentially must determine the optimum mass of each absorber to ensure the suppression of different vibration modes. An established design for a single-degree-of-freedom system can then be applied to an individual absorber.

1.2 *Dynamics of human arm*

Human upper limbs are part of a complex, dynamic system, and their dynamics need to be fully understood before a successful control strategy can be implemented. If we examine the human limb from the point of view of dynamics, we realise that every degree of freedom (DOF) is actuated by more than two driving elements (muscles). For example, five muscles, the biceps brachii, brachialis, brachioradialis, pronator teres and extensor carpi radialis longus, take part in elbow flexion (CNOCKAERT *et al.*, 1975).

Dynamic modelling of the arm is vital to understanding of the muscle activation related to arm movement. It provides a platform upon which different hypotheses on central neural control mechanisms (e.g. the 'Equilibrium-point' hypothesis or 'λ-model') can be verified. Experiments can be designed accordingly, and muscle activities can be recorded (by using the EMG technique, for example). The data can then be compared with the results obtained from numerical simulation of the model.

Such models are of interest to biomechanical studies of the attenuation of pathological tremors and the design of prostheses for the arm and in sports, such as tennis and swimming. Using mathematical modelling, further knowledge of the principles of musculoskeletal system control can be obtained. The first question is how to model this complex anatomical structure so that relevant features can be simulated. Then, suitable mathematical approaches have to be provided for model investigation.

A brief survey of the literature reveals that the human arm has been commonly modelled as a double-jointed, two-dimensional dynamic system (JACKSON and JOSEPH, 1978; FLANAGAN *et al.*, 1992; CORRADINI *et al.*, 1992). In almost all the published papers, the bones and the soft tissues belonging to them were modelled as rigid bodies, where their centre of gravity remained unchangeable in the process of motion. In addition, the joints were modelled as ideal, frictionless kinematic joints with strictly fixed axes or centres of rotation. In the lumped-mass planar model developed by JACKSON and JOSEPH (1978), motion in the sagittal plane was studied where the upper arm and the forearm were represented by straight, pivoted rods. The Lagrangian method was adopted to derive the dynamic mathematical model. In this case, once muscular torques, resistive torques and accelerations of the shoulder are available, the motion of the arm (forward mechanism) can be determined. Similar 2D models were also presented by FLANAGAN *et al.* (1992) and CORRADINI *et al.* (1992).

Various 3D models of a whole or partial upper limb have been also developed over the last decade. LAMAY and CRAGO (1996) developed a dynamic model with four DOFs, where the shoulder and hand functions were not represented. RAIKOVA (1992) presented a more sophisticated model with seven DOFs. The dynamic model was derived using the Newton–Euler method. Indeterminate problems for muscular forces and joint reactions were studied, based on the derived model. As the above

approaches do not separate the changeable muscle forces from the model itself, the construction process has to be repeated whenever a new (or existing) muscle group is included in (or excluded from) the investigation. In contrast, models developed with the Lagrangian method do not have this drawback, as the new variable muscle forces can be incorporated into the model even after it has been built.

YANG *et al.* (1993) developed a seven DOF model where the arm was viewed as three linked pendulums. It was assumed that the mass of each segment was located at the distal end of the segment, and the geometry of each segment was described only by its length. This simplification could result in poor accuracy. To improve the model, distributed mass should be considered. In this study, a planar human arm model, with two DOFs and with distributed mass and inertia, is considered, and the Lagragian approach is used to derive the equations of motion.

2 Biomechanical arm model

2.1 *Two DOF model*

Describing the kinematics and dynamics of the arm using Lagrangian dynamics (WILLIAMS, 1996), a representative biomechanical model with two DOFs was developed (Fig. 1). The body's trunk was considered to be fixed, and connections were made at the shoulder joint and elbow joint (idealised as two pin joints). The model was used to investigate dynamic response and control schemes under external force.

This model described planar motion: flexion/extension in the shoulder joint and elbow joint. It consisted of two rigid segments and two joints representing the shoulder and elbow. The forearm and hand were considered to be one segment. Movements were produced by three pairs of antagonistic muscles: the single joint (pair 1), the elbow joint (pair 2) and the bi-articular muscles (pair 3) that cross both the shoulder and elbow joints (LAN, 1997).

Assuming small angular displacements and neglecting the higher-order terms, the non-linear equations of motion can be linearised in the neighbourhood of the point of stable equilibrium (i.e., here, $\theta_1 = 45^\circ$ and $\theta_2 = 90^\circ$) as

$$[\boldsymbol{M}]\{\ddot{\theta}\} + [\boldsymbol{C}]\{\dot{\theta}\} + [\boldsymbol{K}]\{\} = \{\boldsymbol{F}\}\sin(\omega t) \tag{1}$$

where $[\boldsymbol{M}]$, $[\boldsymbol{C}]$, $[\boldsymbol{K}]$, $\{\boldsymbol{\theta}\}$ and $\{\boldsymbol{F}\}$ represent the symmetric mass, damping and stiffness matrices and the angular displacement and excitation force vectors, respectively. Consequently, linear vibration theory can then be used. Here,

$$\boldsymbol{M} = \begin{bmatrix} M_{11} & M_{12} \\ M_{21} & M_{22} \end{bmatrix} \quad \boldsymbol{K} = \begin{bmatrix} k_1 + k_3 & k_3 \\ k_3 & k_2 + k_3 \end{bmatrix}$$
$$\boldsymbol{C} = \begin{bmatrix} c_1 + c_3 & c_3 \\ c_3 & c_2 + c_3 \end{bmatrix} \tag{2}$$

where

$$M_{11} = (I_1 + m_1 a_1^2) + (I_2 + m_2 a_2^2) + m_2 l_1^2 + m_b(l_1^2 + l_2^2) + m_3(l_1^2 + l_3^2)$$
$$M_{12} = (I_2 + m_2 a_2^2) + m_b(l_2^2) + m_3(l_3^2)$$
$$M_{21} = M_{12}$$
$$M_{22} = (I_2 + m_2 a_2^2) + m_b(l_2^2) + m_3(l_3^2)$$

I_1 and I_2 are moments of inertia at the centre mass of the upper arm and forearm; m_1 and m_2 are the masses of the upper arm and forearm; l_1, l_2, l_3 and l_a are the lengths of the upper arm and forearm and the distances from the absorber's centre of gravity and the absorber's joint to the elbow joint, respectively; a_1 and a_2 are the distances from the proximal joint to the centre of mass of the upper arm and forearm; F_1 and F_2 are the external torques

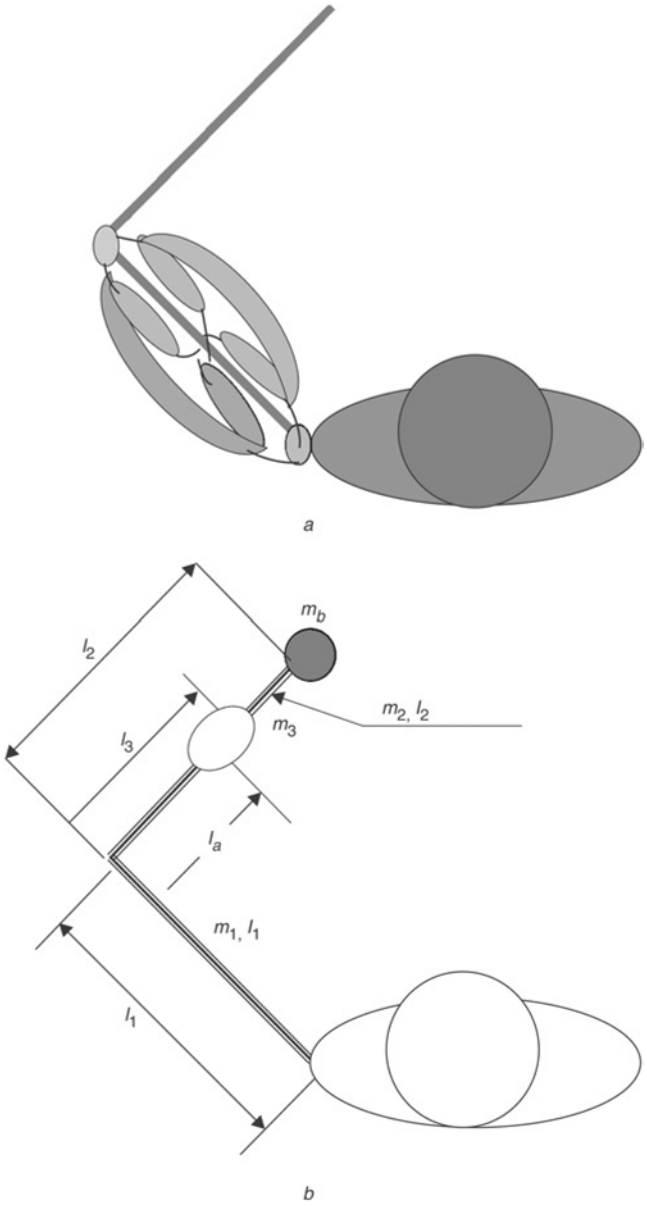

Fig. 1 *(a) Diagram of planar, two-segment model of arm; (b) schematic diagram of arm model*

acting at the shoulder and elbow joints, respectively; θ_1 and θ_2 represent the angles of flexion at the shoulder and elbow, and k_i and c_i are the net stiffness and damping coefficients of each pair of muscles. The assumption was made that the bi-articular muscles have equal moment arms at both joints. It was also assumed that the damping coefficients of the muscles are linear and proportional to stiffness, related by the constants (MAIA and SILVA, 1997). In this model, two other point masses, m_b and m_3, were also included to reflect the presence of the excitation and controller devices, respectively, as will be discussed in detail, later in this paper.

2.2 *Numerical simulation*

To determine appropriate controller stiffness and damping, the mechanical behaviour of the arm in response to transient perturbations was studied first. It is known that the stiffness of a muscle increases with the level of its activation (CANNON and ZAHALAK, 1982). The effect that a change in muscle stiffness has on the damping and stiffness coefficients contributing to joint torque depends on whether or not that muscle crosses more than one joint. Thus increased activation of muscles such as brachioradialis and brachialis, which do not cross the shoulder joint,

would serve to increase k_2 without affecting k_3, whereas increased activation of bi-articular muscles such as the biceps would lead to an increase in both k_2 and k_3. Theoretically, there is a possibility that each of the stiffness coefficients k_1, k_2 and k_3 could be regulated independently. Numerical simulations of the arm motion were carried out and reported by LI (2000), in which cross-joint stiffness k_3 was varied, while the other stiffness terms k_1 and k_2 were kept fixed. It was shown that the impulse forces on the upper arm resulted in angular motions at the shoulder and elbow that were oppositely directed: flexion at the shoulder and extension at the elbow. The cross-coupling stiffness k_3 decreased the effective stiffness at the shoulder and elbow, and, consequently, the amplitude of the angular oscillations at both joints increased as k_3 was increased. In normal people, the inappropriately oscillating movements are damped out. For patients with Parkinson's disease, it is assumed that reduced muscle tone causes a limb to behave like an underdamped mechanical system (LI, 2000).

Based on the modal analysis (MAIA and SILVA, 1997), the natural frequency ω_i of the undamped system and the corresponding eigenvector $\{\boldsymbol{\phi}_i\}$ were first calculated. The matrix of eigenvectors $[\boldsymbol{P}]$ was then evaluated and was used to decouple (1) into separate second-order equations in a modal co-ordinate

Table 1 Two DOF system topology

Parameter	Value	Unit	Definition
l_1	0.30	m	length, upper arm
l_2	0.45	m	length, forearm
l_3	0.45	m	length, absorber device arm
d_1	0.06	m	outer diameter
d_2	0.05	m	inner diameter
m_1	1.45	kg	shoulder mass
m_2	2.18	kg	elbow mass
M_A	0.30	kg	total absorber mass
m_b	0.49	kg	excitation device
k_1	180	Nm	shoulder spring stiffness
k_2	250	Nm	elbow spring stiffness
k_3	set to 0.0	Nm	bi-articular spring stiffness
c_1	$(0.001)k_1$	Nm · s	shoulder joint damping coefficient
c_2	$(0.002)k_2$	Nm · s	elbow joint damping coefficient
$F_1 = 0$, and $F_2 = 10$		Nm	external harmonic torques

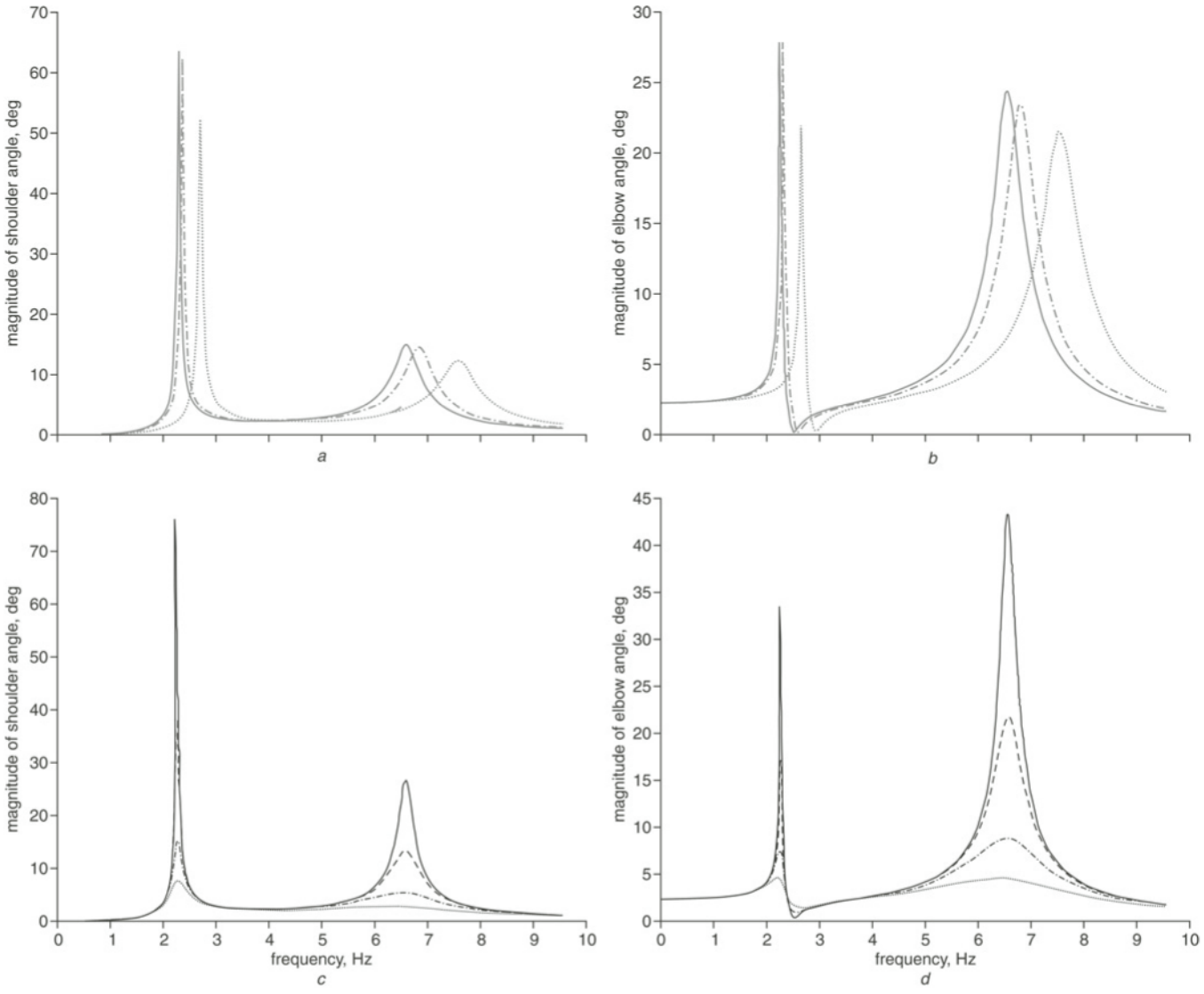

Fig. 2 *Magnitude (deg) of (a) θ_1; (b) θ_2; (—) All arm, absorber and driving motor masses are included;) (-·-·-) arm and driving motor masses are included, but absorber mass is excluded ($m_a = 0$); (· · · ·) total absorber mass and driving motor are excluded ($m_a = 0$, $m_b = 0$); (c) $|\theta_1 = \alpha_{12}F_2|$ (d) $|\theta_2 = \alpha_{22}F_2|$ (deg), for different damping coefficients; (—) $c_1 = c_2 = (0.001)k_1$, and $c_3 = 0$; (– – –) $c_1 = c_2 = (0.002)k_1$, and $c_3 = 0$; (-·-·-) $c_1 = c_2 = (0.005)k_1$, and $c_3 = 0$; (· · · · · ·) $c_1 = c_2 = (0.010)k_1$, and $c_3 = 0$*

system. They could then be solved and analysed using single-degree-of-freedom methods, where ω is the tremor driving frequency and

$$[\boldsymbol{I}]\{\ddot{r}\} + [\boldsymbol{P}]^T[\tilde{\boldsymbol{C}}][\boldsymbol{P}]\{\dot{r}\} + [\boldsymbol{P}]^T[\tilde{\boldsymbol{K}}][\boldsymbol{P}]\{r\} = \{f\}\sin(\omega t) \tag{3}$$

where

$$[\tilde{\boldsymbol{C}}] = [\boldsymbol{M}]^{-1/2}[\boldsymbol{C}][\boldsymbol{M}]^{-1/2} \quad [\tilde{\boldsymbol{K}}] = [\boldsymbol{M}]^{-1/2}[\boldsymbol{K}][\boldsymbol{M}]^{-1/2}$$
$$[f] = [\boldsymbol{P}]^T[\boldsymbol{M}]^{-1/2}\{F\}$$

and $\{\boldsymbol{r}(t)\} = [\boldsymbol{P}]^T[\boldsymbol{M}]^{1/2}\{\boldsymbol{\theta}\}$ represents the modal co-ordinate vector. The two decoupled modal equations can be written as

$$r_1 = \frac{f_1}{\sqrt{(\omega_1^2 - \omega_{dr}^2)^2 + (2\zeta_1\omega_1\omega_{dr})^2}} \times \cos\left(\omega_{dr}t - \tan^{-1}\frac{2\zeta_1\omega_1\omega_{dr}}{\omega_1^2 - \omega_{dr}^2}\right)$$

$$r_2 = \frac{f_2}{\sqrt{(\omega_2^2 - \omega_{dr}^2)^2 + (2\zeta_1\omega_2\omega_{dr})^2}} \times \cos\left(\omega_{dr}t - \tan^{-1}\frac{2\zeta_2\omega_2\omega_{dr}}{\omega_2^2 - \omega_{dr}^2}\right) \tag{4}$$

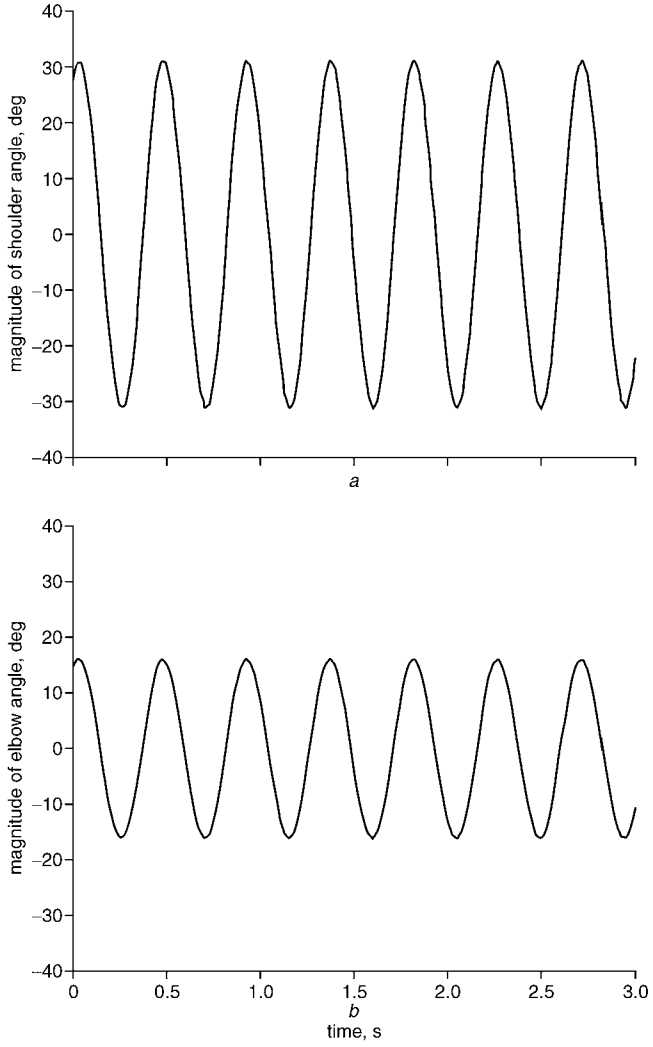

Fig. 3 *Two DOF system time responses for driving frequency $\omega_{dr} = 2.237$; (a) $|\theta_1|$ = shoulder angle; (b) $|\theta_2|$ = elbow angle (deg)*

where $\zeta_1 = \tilde{C}(1, 1)/2\omega_1$, and $\zeta_2 = \tilde{C}(2, 2)/2\omega_2$. Then, the solution is obtained from $\{\boldsymbol{\theta}(t)\} = [\boldsymbol{S}]\{\boldsymbol{r}(t)\}$, where $S = M^{-1/2}P$. Based on the two-DOF system topology presented in Table 1, the first two natural frequencies of the system and the corresponding modal matrix were found to be

$$\omega_1 = 2.27 \text{ (Hz)} \quad \text{and} \quad \omega_2 = 6.59 \text{ (Hz)}$$
$$[\boldsymbol{P}] = \begin{bmatrix} -0.872 & 0.490 \\ -0.490 & -0.872 \end{bmatrix} \tag{5}$$

It is important to note that, for simplicity in the fabrication of the experimental model, the bi-articular stiffness k_3 is omitted throughout this paper. The frequency response functions (FRFs) for θ_1 and θ_2, and for different scenarios (i.e. including only arm inertia, arm and driving device inertia, and, finally, arm, driving and absorber device inertia terms) are shown in Figs 2*a* and *b*. A frequency-domain parameter study for different damping coefficients was also carried out. As shown in Figs 2*c* and *d*, higher damping coefficients resulted in smaller amplitudes at resonance.

Substituting $[\boldsymbol{P}]$, ζ, ω_i and c_i into (4) and including all the inertia terms, the angular displacements in the physical co-ordinates were calculated. The 2 DOF system time response was studied for different inertia combinations discussed earlier. Figs 2*a* and *b* show the magnitudes of θ_1 and θ_2 as a function of time for the case including all the arm, driving and absorber device inertia terms. Based on the natural frequencies and modes of vibration of the system and the frequency responses (see (4) and (5)), the first vibration mode represented the case where the shoulder vibrates with a larger amplitude compared with the forearm. This fact was also confirmed by the time response (Fig. 3), where the system was excited with $\omega_{dr} = 2.237$ Hz, close to ω_1. Re-evaluating the system time response for different driving frequencies led to $\theta_1 < 1^\circ$ and $\theta_2 < 3^\circ$, for $\omega_{dr} = 1.5$ Hz, and $\theta_1 < 6^\circ$ and $\theta_2 < 3^\circ$, for $\omega_{dr} = 5.5$ Hz, respectively. In other words, θ_1 and θ_2 could respond differently (i.e. the amplitude of θ_1 can be larger or smaller than θ_2).

3 Tremor suppression strategy

3.1 *Dynamic analysis*

As was stated earlier, in general, tremor control requires that motion in all joints be controlled simultaneously. However, for the sake of simplicity and practical implementation, in this research, we used only one absorber. To investigate control performance, our study focused on the frequency response function and time response of uncontrolled and controlled vibrations of the human arm model, using a vibration absorber. The dynamic model of the arm with the vibration absorber is illustrated in Fig. 4. Assuming a pendulum absorber model (see Fig. 4), incorporating the motor mass and the absorber mass, and linearisation at $\theta_1 = 45^\circ$ and

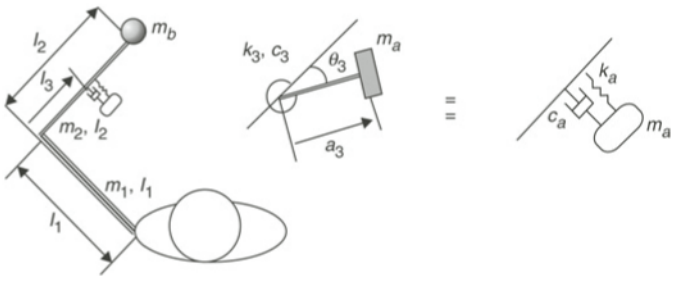

Fig. 4 *Two DOF arm model, with vibration absorber modelled as 3rd DOF, and dynamic absorber and equivalent pendulum model*

$\theta_2 = 90°$, the governing equations of motion have the same form as (1), where $[\boldsymbol{M}]$, $[\boldsymbol{C}]$ and $[\boldsymbol{K}]$ matrices are

$$\boldsymbol{M} = \begin{bmatrix} M_{11} & M_{12} & M_{13} \\ M_{21} & M_{22} & M_{23} \\ M_{31} & M_{32} & M_{33} \end{bmatrix} \quad \boldsymbol{K} = \begin{bmatrix} k_1 & & \\ & k_2 & \\ & & k_3 \end{bmatrix}$$
$$\boldsymbol{C} = \begin{bmatrix} c_1 & & \\ & c_2 & \\ & & c_3 \end{bmatrix} \tag{6}$$

where

$$\begin{aligned} M_{11} &= (I_1 + m_1 a_1^2) + (I_2 + m_2 a_2^2) + m_2 l_1^2 + m_b(l_1^2 + l_2^2) \\ &\quad + m_3(l_1^2 + l_3^2) + m_a(l_1^2 + l_a^2 + a_3^2 + 2l_a a_3) \\ M_{12} &= (I_2 + m_2 a_2^2) + m_b(l_2^2) + m_3(l_3^2) \\ &\quad + m_a(l_a^2 + a_3^2 + 2l_a a_3) \\ M_{13} &= m_a(a_3^2 + l_a a_3) \\ M_{21} &= M_{12} \\ M_{22} &= (I_2 + m_2 a_2^2) + m_b(l_2^2) + m_3(l_3^2) \\ &\quad + m_a(l_a^2 + a_3^2 + 2l_a a_3) \\ M_{23} &= M_{13} \\ M_{31} &= M_{13} \\ M_{32} &= M_{23} \\ M_{33} &= I_3 + m_a a_3^2 \end{aligned}$$

I_3 is the moment of inertia of the absorber; m_a represents the absorber vibrating (proof) mass; l_3 and l_a are the distances from the absorber's centre of gravity and the absorber's joint to the elbow joint, respectively; a_3 represents the absorber's length (i.e. $l_a + a_3 =$ distance from the proof mass to the elbow joint); θ_3 represents the angle of flexion of the proof mass (m_a). The rest of the parameters are the same as already presented. As before, we have made the assumptions that the damping coefficients of the muscles are linear and proportional to stiffness, related by the constants. If the modal transformation approach is applied, the equations of motion can then be decoupled to three second-order equations in a modal co-ordinate system. Then, the same approach as applied to the two DOF system leads to the frequency and time responses of this system. The frequency response functions (FRFs) for the DOFs of the system are then obtained from

$$\theta_i = |\alpha_{ij}||F_j| \tag{7}$$

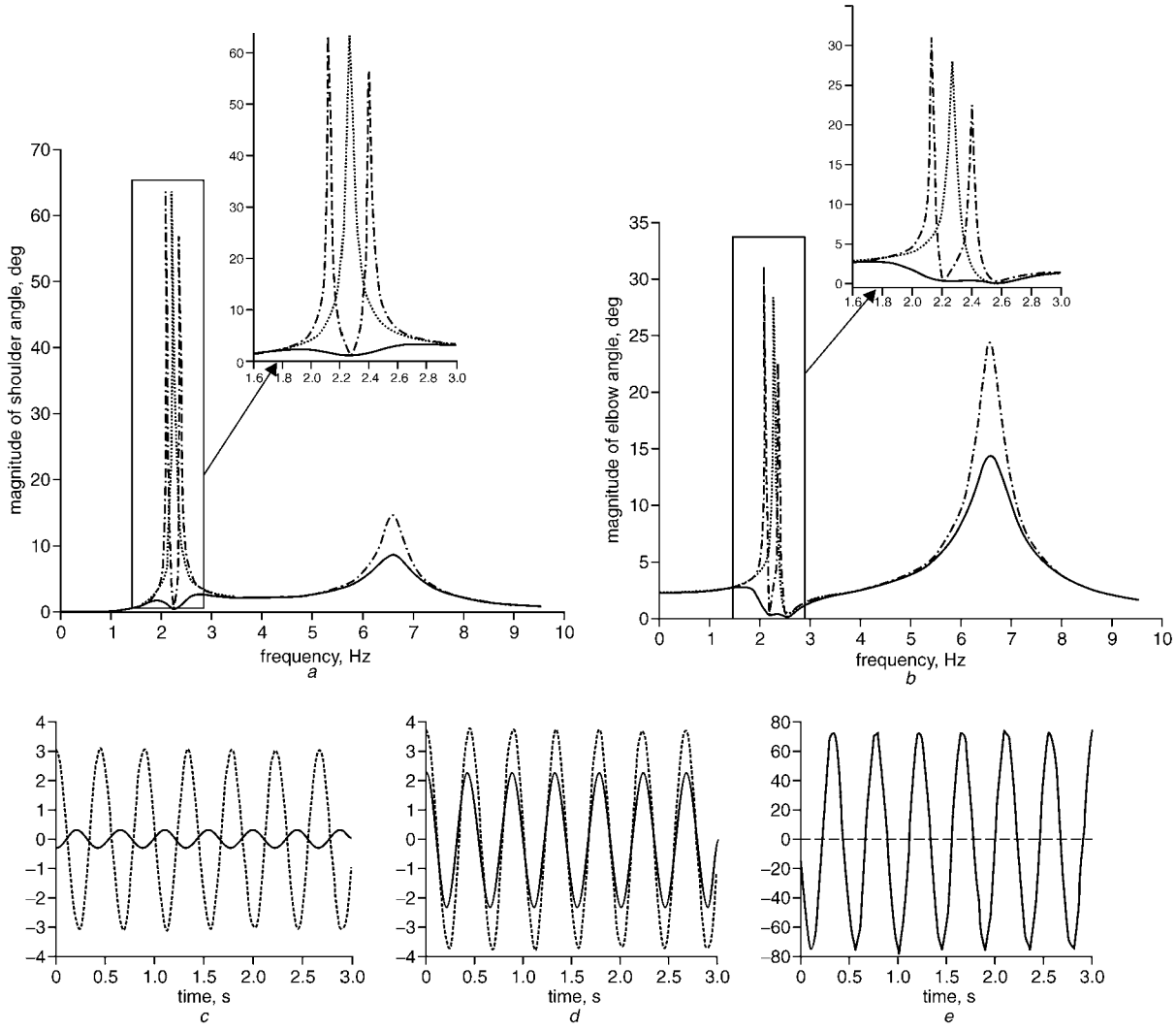

Fig. 5 *Magnitude of uncontrolled and controlled vibrations (deg): (a) shoulder angle; (b) elbow angle; for $F_{dr} = 10$ Nm, and $c_1 = (0.001)k_1$; $c_2 = (0.002)k_2$; and different absorber damping coefficients c_3; (· · · · · ·) uncontrolled (two DOF system); (-·-·-) controlled system (TVA tuned at $\omega_a = 2.755$ Hz) and $c_3 = 0$; (—) controlled system (TVA tuned at $\omega_a = 2.755$ Hz) and $c_3 = (0.05)k_3$; (c) shoulder θ_1, (d) elbow θ_2 and (e) absorber θ_3 time responses, respectively, for uncontrolled and controlled vibrations of arm for $F_{dr} = 10$ Nm, $\omega_{dr} = 2.24$ Hz, $\omega_a = 2.755$ Hz, and damping coefficients $c_1 = (0.001)k_1$, $c_2 = (0.001)k_2$ and $c_3 = (0.05)k_3$; (---) uncontrolled (two DOF) system; (——) controlled system*

where

$$\alpha_{ij} = A_{ij} + iB_{ij} \Rightarrow \left|\alpha_{ij} = \frac{\theta_i}{F_j}\right| = \frac{\sqrt{A_{1_{ij}}^2 + B_{1_{ij}}^2}}{\sqrt{A_2^2 + B_2^2}}$$

$$A_{1_{12}} = \omega^2(M_{12}k_3 - \omega^2 M_{12}M_{33} + \omega^2 M_{13}M_{32})$$

$$A_{1_{22}} = (k_1k_3) - \omega^2(k_1M_{33} + k_3M_{11} + c_1c_3) + \omega^4(M_{11}M_{33} - M_{13}M_{31})$$

$$A_{1_{23}} = \omega^2(M_{23}k_1 - \omega^2 M_{23}M_{11} + \omega^2 M_{13}M_{21})$$

$$B_{1_{12}} = \omega^3 M_{12}c_3$$

$$B_{1_{22}} = \omega(k_1c_3 + c_1k_3) - \omega^3(M_{11}c_3 + c_1M_{33})$$

$$B_{1_{23}} = \omega^3 M_{23}c_1$$

$$A_2 = (k_1k_2k_3) - \omega^2(M_{11}k_2k_3 + M_{22}k_1k_3 + M_{33}k_1k_2 + k_1c_2c_3 + k_2c_1c_3 + k_3c_1c_2) + \omega^4(M_{11}M_{33}k_2 + M_{11}M_{22}k_3 + k_1M_{22}M_{33} - k_1M_{23}M_{32} - M_{21}M_{12}k_3 - M_{31}M_{13}k_2 + M_{11}c_2c_3 + M_{22}c_1c_3 + M_{33}c_1c_2) - \omega^6(M_{11}M_{22}M_{33} - M_{11}M_{23}M_{32} - M_{21}M_{12}M_{33} + M_{21}M_{13}M_{32} + M_{31}M_{12}M_{23} - M_{31}M_{13}M_{22})$$

$$B_2 = \omega(k_1c_2k_3 + c_1k_2k_3 + k_1k_2c_3) + \omega^3(M_{11}(k_2c_3 - c_2k_3) - M_{22}(c_1k_3 + k_1c_3) - M_{33}(k_1c_2 + c_1k_2) - (c_1c_2c_3)) + \omega^5(c_3(M_{11}M_{22} - M_{21}M_{12}) + c_1(M_{22}M_{33} - M_{23}M_{32}) + c_2(M_{11}M_{33} - M_{31}M_{13}))$$

and $\alpha_{ij} = \alpha_{ji}$. α_{ij} are called the receptance transfer functions.

The absorber can then be designed so that the vibration amplitude of any specific DOF tends to zero. We can then evaluate (tune) the absorber parameters so that the real part of the numerator, in the corresponding receptance expression, approaches zero. The uncontrolled and controlled FRFs for the shoulder (θ_1) and elbow (θ_2) vibrations, for $F_{dr} = 10$ Nm, $c_1 = (0.001)k_1$ and $c_2 = (0.002)k_2$, and for different absorber damping coefficients c_3, are demonstrated in Figs 5*a* and *b*. It was shown by LI (2000) that the absorber performance improves as absorber (proof) mass increases. Here, the simulations are performed based on $m_a = 0.13$ kg, as reported by LI (2000).

Comparing Figs 5*a* and *b*, it can be observed that the FRF numerical simulation, for both shoulder and elbow angles, represents two peaks at the resonance frequencies of the uncontrolled arm, whereas the controlled system shows three peaks. As can be seen, the first peak has been transformed into two peaks, where they have been shifted slightly away from the first natural frequency of the uncontrolled system (i.e. changing a two DOF system to a three DOF one with modified inertia effects). This may explain the difference in the first natural frequency between the uncontrolled system and the controlled system. Although the vibration absorber adds another peak to the system, the resonant responses are well damped compared with those of the original system. If we fix the absorber damping coefficient $c_3 = 0$, the peaks are almost zero, but only for a single point. If we increase c_3, however, a wide range of frequency can be controlled, but it is no longer possible to eliminate the vibrations completely.

Figs 5*c–e* indicate the time response of the three DOF arm model when the system is excited with a frequency close to its first natural frequency ($\omega_{dr} = 2.24$ Hz), and the absorber is tuned to $\omega_a = 2.755$ Hz. It can be observed that the amplitudes of the tremor are greatly attenuated when the absorber is activated. The results also confirm the validity of the proposed model and the great effectiveness of the suggested vibration absorber to control tremor of the two DOF planar arm.

4 Analysis of the experimental system

The numerical simulation presented in the preceding Section showed the applicability of the theory and proposed controller. Experimental studies were then carried out to move closer to reality, to verify the practical applicability of the system and to assess the effectiveness of the controller. The experimental set-up is briefly presented, followed by measurements of tremor, without control and with a TVA controller. Experiments were also carried out to determine the optimum TVA position with reference to the performance of the controller. Finally, simulation results are presented and compared with the experimental results to ascertain the accuracy of the experimental model.

A dynamic replica of a two DOF experimental arm was designed and fabricated for use in the laboratory environment. A small DC motor with unbalanced mass was incorporated into the arm to provide the excitation force and eventually to generate tremor. A passive tuned vibration absorber (TVA) was designed as the controller to suppress tremor in the experimental arm.

4.1 *Experimental apparatus*

The model is shown in Fig. 6. The two DOF planar experimental model consists of two pairs of springs that replace antagonistic muscles in the biomechanical model: pair 1 and pair 2 have two sets of springs that are in parallel with shoulder and elbow muscles, respectively. These pairs are in equilibrium when the system is set to a horizontal position. The oscillations of the arm model make the springs perform a push–pull function. Spring mounts were designed to hold the springs. The springs can be adjusted to produce different arm postures (Fig. 6).

4.2 *TVA design*

The TVA consists of three main parts: the absorber mass, tuning structure and body. The tuning structure includes a beam spring and a guide slider, and its body includes the case and support cover and is attached to the forearm. The TVA is manually tuned to the tremor's frequency to absorb or extract tremor out of the oscillatory arm by adding a physical spring-mass-damper system.

The absorber mass (also called the proof mass) is used to dissipate vibration energy. The TVA has to be light, small and simple to adjust. Its total mass should be below 10% of the arm weight (e.g., for a person with a weight of 75 kg, the mass of the arm is approximately 3.75 kg (LI, 2000)). As the designed experimental model has a total mass of 3.63 kg, the total mass of the TVA was limited to 0.3kg. To prevent interference between the absorber mass and body, the mass was designed as a half cylinder (with a radius of 20 mm and a height of 26 mm), leading to an absorber mass of 0.13 kg. To minimise

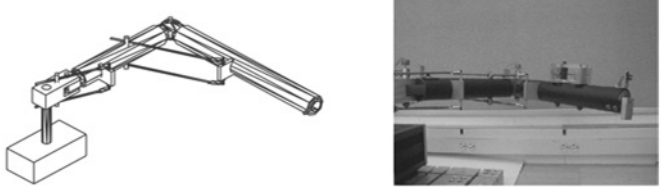

Fig. 6 *Final design of experimental arm and front view of experimental arm*

the machining efforts and also the volume, brass was used for the absorber mass, as brass has a relatively higher density (8.5×10^3 kg m^{-3}) than other common metals.

A steel 'beam' spring (Young's modulus $E = 2.07 \times 10^{11}$), of dimensions $85 \times 4 \times 0.5$ mm, was used as the variable stiffness element of the absorber, providing an excellent bending property to transverse vibration. An adjustable plastic slider was designed to vary the effective length of the beam spring, providing the absorber's variable natural frequency. Owing to the practical difficulties, damper elements were not used in the absorber. However, owing to the little damping provided by the beam spring, amplitudes of absorber mass were acceptable. Moreover, too much damping could inhibit tremor reduction. The body of the TVA supported the adjusting slider, beam spring and damper. The body of the TVA had a groove that guided the slider with minimum lateral play. The body of the TVA was bolted to the forearm, and the adjusting screw tightened the slider against the cover after tuning to resonance frequency.

For both the elbow joint and shoulder joint, displacements were measured with two low damping potentiometers* mounted at the joint axes. These small, lightweight sensors could be mounted directly onto the supporting bracket and connected with joint shafts using couplings. The experimental arm was triggered by unbalanced forces generated by the motor.

Excitation frequencies were measured using a slotted optical switch sensor (model H21A1) that was linked to a digital frequency counter. A DC power supply† was used to drive the DC motor: the output voltage of the power supply could be adjusted to change the speed of the motor, i.e. driving frequency. The other DC power supply was used to power the potentiometers and optical switch sensor. The output signals from the potentiometer were passed through a low-pass filter‡ (30 Hz cutoff frequency) to remove high-frequency noise. Output from the filter was sent to a dynamic signal analyser** that recorded the time response to sinusoidal excitation of constant frequencies ranging from 0.5 to 10 Hz. A Matlab code was written to transfer data from the dynamic signal analyser to the computer. The data were displayed and printed using Matlab. Fig. 7 shows the instrumentation and the connectivity.

The experimental frequency response plots are shown in Fig. 8 to illustrate the effectiveness of the controller at the shoulder and the elbow joints. The lines with circles represent the experimental results without tremor control, and the lines with asterisks represent the experimental results with tremor control. These Figures indicate that the TVA can selectively attenuate tremor within the frequency range of 1–10 Hz. Fig. 8*a* demonstrates that the TVA can almost stop tremor of the shoulder joint from 4.0 to 7.0 Hz. Two peaks of the uncontrolled system correspond to the natural frequencies, 2.7 Hz and 8.0 Hz. The natural frequencies of the controlled system are 2.5 Hz and 8.0 Hz. In the controlled case, there is a shift in the first natural frequency of the system. It is due to the change in the effective inertia of the whole system and is supported by the theoretical facts previously explained in Section 3. However, as can be seen, the absorber has very little effect on the second natural frequency, 8.0 Hz. The frequency response plots are shown in Fig. 8*b* to illustrate the effectiveness of the controller at the elbow joint.

Fig. 8*b* indicates that the controller nearly eliminates tremor in the elbow joint from 3.4 to 5 Hz. Although the amplitude of the tremor increases when frequency increases from 5 to 7 Hz, the controlled amplitudes are smaller than 0.20 deg in the elbow joint. The natural frequencies of the controlled system

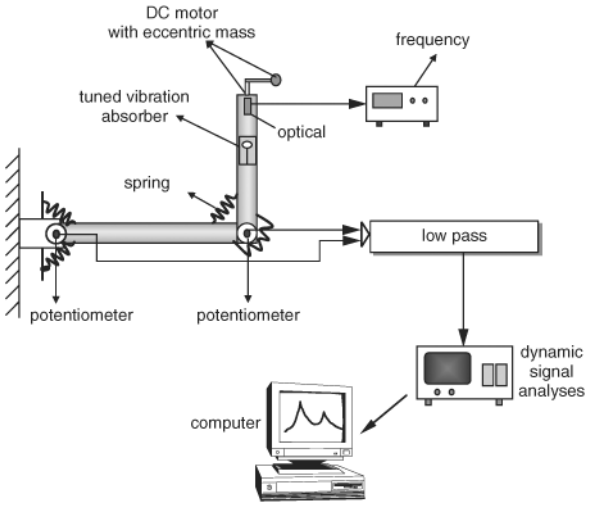

Fig. 7 *Experimental instrumentation*

are 2.5 Hz and 8.0 Hz, which are identical to those in Fig. 8*a*. This Figure also shows the same difference in the first natural frequency between the uncontrolled system (2.7 Hz) and the controlled system (2.5 Hz). The frequency responses measured in the shoulder and elbow joints have identical natural frequencies for both uncontrolled and controlled cases. This demonstrates that the measurement of the frequency response is accurate. Figs 8*a* and *b* also show the fact that this controller is very effective in the frequency range of 3.4–7.0 Hz.

The performance of the TVA at the first resonant frequency, 2.7 Hz, is illustrated in Fig. 9 by comparison of the time responses both with and without control. At steady state, the

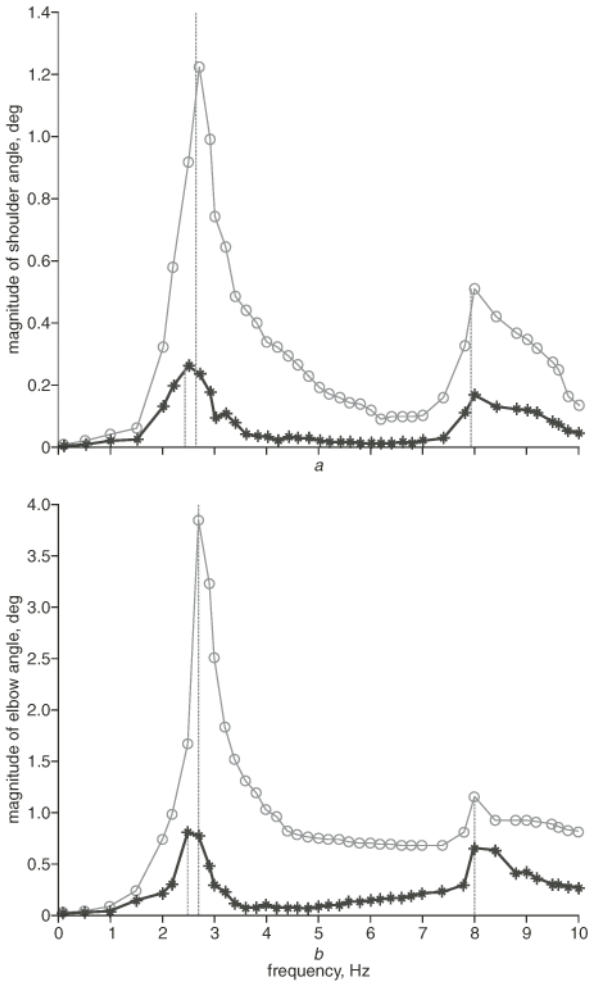

Fig. 8 *Experimental frequency response results: (a) shoulder joint; (b) elbow joint (-○-○-○) Uncontrolled; (-*-*-*-) controlled*

*Spectral model 158-146-02

†Philips PE 1542

‡Hewlett Packard 5489A

**Hewlett Packard 35670A

TVA achieved a 14.27 dB and 13.93 dB reduction in the tremor amplitude of the shoulder and elbow motion in the experimental arm. For the second resonance, initially, the vibration absorber was mistuned, and the experimental arm was then excited at a frequency of 8.0 Hz. The controller was then retuned to suppress the tremor for the second resonance. It was observed that, at steady state, the TVA achieved a 9.7 dB and 4.95 dB reduction in the tremor amplitude of the shoulder and elbow, respectively. Therefore this controller is more effective for lower frequencies. The difference in effectiveness is probably caused by the out-of-plane bending and whirling of the experimental arm at higher frequencies. The out-of-plane bending and whirling results in disturbance to the controller and potentiometers. This, in turn, would affect the performance of the controller.

The experimental FRF results shown in Figs 8*a* and *b* are similar to those obtained from numerical simulations already presented in Figs 5*a* and *b*. Even though the amplitudes and the second natural frequency were found to be different from those obtained from simulations, the results were well matched qualitatively. These differences can be attributed to the difference between the theoretical stiffness values assumed for the shoulder and elbow joints, as well as the assumed damping coefficients, and those resulting during the implementation of the experimental apparatus. Similar conclusions can also be reached comparing the numerical simulation and experimental time-domain studies. Generally speaking, the experimental results were qualitatively consistent with the theoretical analysis, and simulation and experimental results showed good correlation.

4.3 *Variation of the controller position*

A parametric study was carried out to investigate the effect of varying the position of the controller. The displacement of the TVA from the end of the forearm was changed. Four cases were considered, as illustrated in Fig. 10. Distances of 120, 160, 200 and 240 mm were used.

First, experiments were carried out for lower excitation frequencies. Fig. 11*a* shows the system's uncontrolled and controlled time responses at 3.0 Hz for the TVA at 160 mm from the end of the forearm (position 2). The experiments were also repeated to evaluate the responses for positions 1, 3 and 4 of the controller. In these cases, the TVA produced different reductions in tremor. For this frequency, 3.0 Hz, position 2 clearly appeared to be optimum, suppressing 29.05 dB of tremor amplitude in the elbow joint, as shown in Fig. 11*a*. The tremor amplitudes were decreased by 22.32 and 22.37 dB, when the TVA was located at positions 1 and 3, respectively. This proved that the effectiveness of the controller did not differ at positions 1 and 3. The time response of the TVA at position 4 was attenuated by approximately 20.32 dB.

Similar tests were run for higher excitation frequencies, namely 8.0 Hz, which is the second resonance of the system. The results are shown in Fig. 11*b*. The amplitude of tremor decreased, as expected. As before, the optimum response was obtained at position 2, with a reduction of 10.90 dB. Reductions of 9.51 and 8.67 dB were achieved, when the TVA was located at positions 3 and 4. It is worth noting that the amplitude of the tremor was decreased by 10.90 dB at position 1, but it had a clear beat pattern. This can be attributed to the resulting out-of-plane bending and whirling. The beat pattern would worsen the effectiveness of the controller. The beat phenomenon appeared to be more significant at high frequencies. It would reduce the effectiveness of the TVA to control horizontal tremor, which is measured by potentiometers. It has therefore been demonstrated that optimum control performance is related to the position of the controller and the excitation frequency.

5 Concluding remarks

The goal of this project was to develop a control strategy that could effectively suppress PD tremor of the human arm undergoing involuntary rhythmic oscillations. A dynamic replica of the two DOF arm was designed and fabricated for use in the laboratory environment. The design allows for manipulation of some of its physical attributes, thus providing for future potential parameter investigation. A tuned vibration absorber was

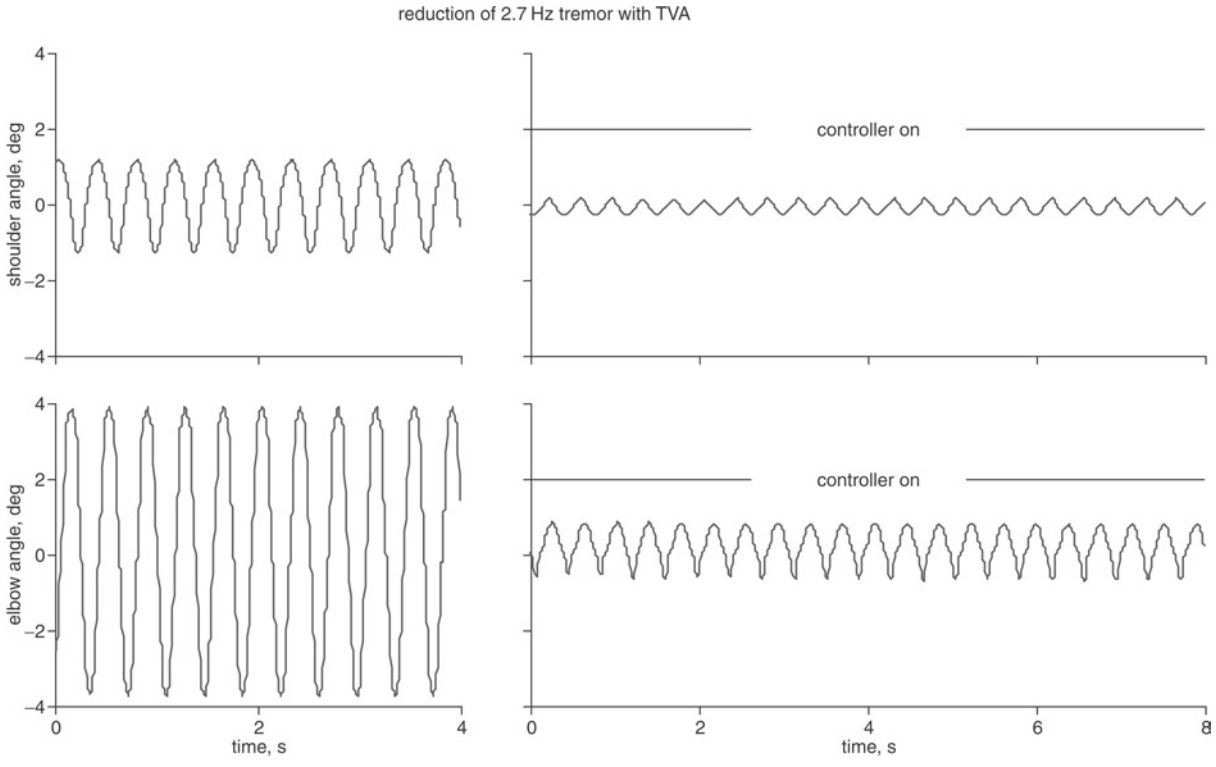

Fig. 9 *Uncontrolled and controlled experimental time responses at 2.7 Hz*

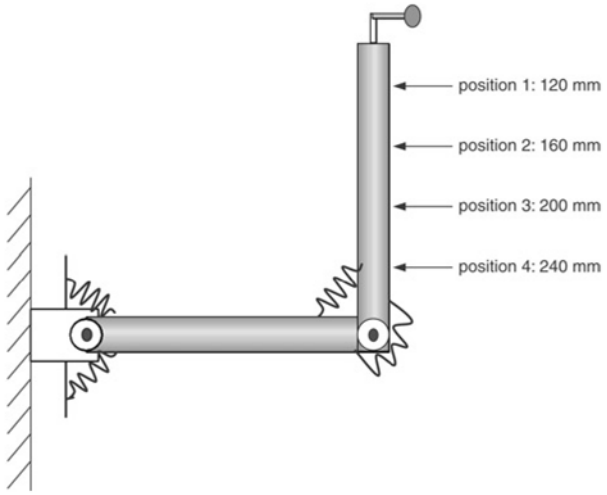

Fig. 10 *Controller placement*

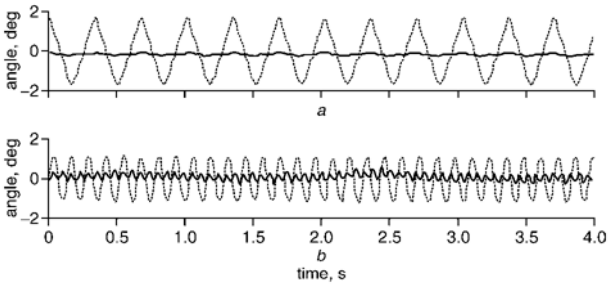

Fig. 11 *Tremor amplitudes of forearm for different TVA positions: (a) at 3.0 Hz; (b) at 8.0 Hz. (– – –) No control;(—) with TVA controller at 160 mm from end of forearm (position 2)*

designed that can be attached to the forearm of the experimental arm. The controller was 'tuned' to the tremor frequency to attenuate tremor. An optimum controller location, which depends on the distance from the end of the forearm, was also obtained.

Experimental results indicate that the TVA is an appropriate device for suppression of tremor associated with Parkinson's disease, as its small mass, when positioned appropriately, can tune out tremor over a broad range of frequencies. In addition, the TVA and its design are very simple compared with existing systems, and it is theoretically feasible to build a single portable device that could benefit a wide range of patients having different, individual tremor frequencies. Finally, the simplified experimental model was found to be sufficiently accurate to permit its use in the design and analysis of this type of controller for the human arm.

Acknowledgments—The authors wish to thank Lei Li, for the design and construction of the experimental apparatus.

This project was supported by grants from NSERC, Canada.

References

ARNOLD, A., and ROSEN, M. (1993): 'Evaluation of a controlled-energy-dissipation orthosis for tremor suppression', *J. Electromyogr. and Kinesiol.*, **3**, pp. 131–148

CANNON, S. C., and ZAHALAK, G. I. (1982): 'The mechanical behaviour of active human skeletal muscle in small oscillations', *J. Biomech.*, **15**, pp. 111–122

CNOCKAERT, J. C., LENSEL, C., and PERTUZON, E. (1975): 'Relative contribution of individual muscles to the isometric contraction of a muscular group', *J. Biomech.*, **8**, pp. 191–197

CORRADINI, M. L., GNTILUCCI, M., LEO, T., and RIZOLATTI, G. (1992): 'Motor control of voluntary arm movement', *Biol. Cybern.*, **57**, pp. 347–360

FLANAGAN, J. R., FELDMAN, A. G., and OSTRY, D. J. (1992): 'Equilibrium trajectories underlying rapid target-directed arm movements', *Tutor. Motor Behav.*, pp. 661–675

GRIFFIN, G. J. (1990): 'Handbook of human vibration' (Academic Press, 1990), p. 182

HALL, W. D. (1996): 'Hand-held gyroscopic device', *US Patent 5562707*

INMAN, D. J. (1996): 'Engineering vibration' (Prentice Hall, 1996)

JACKSON, K. M., and JOSEPH, J. (1978): 'A mathematical model of arm swing during human locomotion', *J. Biomech.*, **11**, pp. 277–289

KARNOPP, D. (1995): 'Active and semi-active vibration isolation', *Special 50th Anniversary Design Issue*, **117**, pp. 177–185

LAN, N. (1997): 'Analysis of an optimal control model of multi-joint arm movements', *Biol. Cybern.*, **76**, pp. 107–117

LEMAY, M., and CRAGO, P. (1996): 'A dynamic model for simulating movements of the elbow, forearm, and wrist', *J. Biomech.*, **29**, pp. 1319–1330

LI, L. (2000): 'Modelling and tremor suppression of human arm with Parkinson's disease'. MSc thesis, Department of Mechancial Engineering, University of Waterloo, Ontario, Canada

MAIA, N. M. M., and SILVA, J. M. M. (1997): 'Theoretical and experimental modal analysis' (Research Studies Press Ltd, Somerset, UK, 1997)

NAGAYA, K., KURUSU, A., IKAI, S., and SHITANI, Y. (1999): 'Vibration control of a structure by using a tunable and an optimal vibration absorber under auto-tuning control', *J. Sound Vibrat.*, **228**, pp. 773–792

PARKINSON, J. (1817): 'An essay on the shaking palsy' (Sherwood, Needly and Jones, London, 1817)

PROCHAZKA, A., ELEK, J., and JAVIDAN, M. (1992): 'Attenuation of pathological tremors by functional electrical stimulation I: method', *Ann. Biomech. Eng.*, **20**, pp. 204–205

RAIKOVA, R. (1992): 'A general approach for modeling and mathematical investigation of the human upper limb', *J. Biomech.*, **25**, pp. 857–867

REPPERGER, D. (1989): 'Accurate hand movement assistance', *US Patent 4842607*

ROSEN, M. (1986): 'Tremor suppressing hand controls', *US Patent 4689449*

SETO, K., and TAKITA, Y. (1984): 'Vibration control in multi-degree-freedom systems, Report 1: On the design of dynamic absorbers', *Trans. Jpn Soc. Mech. Eng.*, **50**, p. 458

SUN, J. Q., JOLLY, M. R., and MORRIS, M. A. (1995): 'Passive, adaptive and active tuned vibration absorbers—A survey', *Trans. ASME*, **117**, pp. 234–240

WILLIAMS, J. H. (1996): 'Fundamentals of applied dynamics' (John Willey & Sons Inc., 1996)

YANG, Y., YAHIA, L., and FELDMAN, A. G. (1993): 'A versatile dynamic model of human arm', *Adv. Bioeng. ASME*, **26**, pp. 36–47

Authors' biographies

FARID GOLNARAGHI is a Mechanical Engineering Professor and Canada Research Chair in Intelligent Mechatronics and Material Systems at the University of Waterloo. He has several patents for pioneering discoveries; authored three books and more than 130 refereed journal papers, conference proceedings and technical reports. He is a Director of the Canadian Society for Mechanical Engineering and holds a number of other key positions in his field.

A. E. PATLA is a Professor in the Department of Kinesiology at the University of Waterloo. His research is in human gait, posture and balance and the effects of pathologies and aging on mobility and balance. He has published over 100 research papers in these areas, he is a co-author on a text on signal processing and modeling for movement science and has edited a book on Adaptability of Human Gait. He was the past president of the Canadian Society of Biomechanics and the International Society for Posture and Gait Research as well as the Executive Editor for Journal of Motor Behavior and Associate Editor of Gait & Posture.

S. M. HASHEMI was a Postdoctoral Fellow at Waterloo in 1998, and has received his PhD from Laval University. He is currently an Assistant Professor at Ryerson University.